Technical Paper

Journal of the Society of Naval Architects of Korea
Vol. 27, No. 4, December 1990
大 韓 造 船 學 會 誌
第27卷 第4號 1990年 12月

Super-Cavitating Flow Problems about Two-Dimensional Symmetric Strut

by

Y.-G. Kim* and C.-S. Lee**

2차원 대칭 스트럿 주위의 초월 공동 유동 문제의 해석

김 영 기*, 이 창 섭**

Abstract

This paper describes a potential-baoed panel method formulated for the analysis cf a super-cavitating two-dimensional symmetri strut. The method employs normal dipoles and sources distributed on the foil and cavity surfaces to represent the potential flow around the cavitating hydrofoil. The kinematic boundary condition on the wetted portion of the foil surface is satisfied by requiring that the total potential vanish in the fictitious inner flow region of the foil, and the dynamic boundary condition on the cavity surface is satisfied by requiring that the potential vary linearly, i.e., the tangential velocity be constant. Green's theorem then results in a potential-based integral equation rather than the usual velocity-based formulation of Hess & Smith type, With the singularities distributed on the exact hydrofoil surface, the pressure distributions are predicted with improved accuracy compared to those of the linearized lifting surface theory, especially near the leading edge. The theory then predicts the cavity shape and cavitation number for an assumed cavity length. To improve the accuracy, the sources and dipoles on the cavity surface are moved to the newly computed cavity surface, where the boundary conditions are satisfied again. This iteration process is repeated until the results are converged.

요 약

본 연구는 표면 양력판 이론을 이용하여 초월 공동이 발생한 2차원 날개의 유동해석을 위한 제반 경계 조건을 검증하고 공동 뒷부분의 모형을 비교 검토한다.

해석해가 존재하는 2차원 대칭 스트럿 주위의 초월 공동 현상을 수치 적으로 해석하여 그 결과를 해석해와 비교함으로써 표면 양력판 이론에 의한 프로펠러 공동 문제 해석의 가능성을 입증하였다. 특히, 공동 뒷부분의 비 선형 닫힘 모형, 타원형 닫힘 모형, 그리고 선형 닫힘 조건을 서로 비교 분석함으로써 공동 문제 해결에서 가장 중요한 공동 닫힘 조건의 영향을 보였다.

발표 : 1989년도 대한조선학회 추계연구발표회('89.11.11)
Manuscript received: November 29, 1989, revised manuscript received: October 16, 1990.
* Student member, Chungnam National Univ.
** Member, Chungnam National Univ.

1. Introduction

As the loading on blades of marine propeller increases, cavitation plays an inceasing role in the unsteady hull forces and also causes severe noise and vibration problems at the stern. In order to control these problems at the stern of a ship and also to design a propeller with a sufficient but not too much cavitation margin, it is necessary to be able to predict the extent and behavior of the cavity on the surface of the propeller blade with much improved accuracy.

Traditional methods predicting the cavitation phenomenon are mostly based on the linearized lifting surface theory.[9] Due to the assumption of thin blade section, the solution near the leading edge of the blade is not so accurate as to give a singular pressure peak there. This unusual negative pressure peak becomes inevitably the source of inaccurate over-prediction of the cavity extent on marine propeller.

To overcome this drawback of the lifting surface theory, the surface panel method is now emerging where the singularities such as sources and normal dipoles are distributed on the exact blade surface rather than on the mean camber surface. (Lee[11], Yang & Jessup[15], Hess & Valarezo[7]) The surface panel method has been applied successfully to the partially cavitating hydrofoil problem by Lee [10].

The cavity on a marine propeller is called a partial cavity or a super-cavity, depending upon whether the after end of the cavity terminates upstream of the trailing edge of the blade or exceeds this edge. Since both types of cavity may occur on a propeller blade simultaneously, it is necessary to acquire capability to predict such cavity behavior equally well.

This paper, continuing the work of Lee[10] on partial cavity problem, describes a solution procedure required to solve the steady super-cavitating flow about a symmetric strut with a blunt base.

Comparing especially the non-linear Riabouchinsky type cavity termination model with the linearized cavity closure condition and elliptical termination model, this paper shows the importance of proper modeling of the cavity termination. Analytical solution for the super-cavity flow around the strut provides a means to evaluate the validity of the numerical procedure of surface panel method and the possibility of its extension to propeller cavitation. Sample calculations are performed to obtain the cavity geometry, pressure distributions, and section drags.

2. Formulation of Boundary Value Problem

Let's consider the unbounded, steady, irrotational flow of an inviscid, incompressible fluid past a cavitating symmetric strut with a blunt base. The total velocity, $\underline{V}$, may be expressed in terms of the total velocity potential, Φ, which is defined using the on-comming velocity, $\underline{U}_\infty$, the position vector, $\underline{x}$, and the perturbation potential, ϕ, as follows,

$$\underline{V}=\nabla\Phi \tag{1}$$

where

$$\Phi=\underline{U}_\infty\cdot\underline{x}+\phi. \tag{2}$$

Conservation of the mass applied to the potential flow gives the Laplace equation as a governing equation, i.e.,

$$\nabla^2\Phi=0, \text{ throughout the fluid.} \tag{3}$$

Motion of the flow can be uniquely defined by imposing the boundary condition on the boundary surfaces, such that

1. Quiescence condition at infinity:

$$\nabla\Phi\to\underline{U}_\infty, \text{ at infinity.} \tag{4}$$

2. Flow tangency condition:

$$\hat{n}\cdot\underline{V}=\frac{\partial\Phi}{\partial n}=0, \text{ on the body surface } S_B \tag{5}$$

where $\hat{n}$ is the outward unit normal vector to the boundary.

The conditions stated above are sufficient to describe the steady motion of a symmetric strut moving in unbounded ideal flow, except a condition constraining the flow with infinity velocity at the trailing edge of the foil.

With the presence of cavity following the strut, we have to apply the kinematic and the dynamic boundary condition on the cavity surface and the cavity closure condition on the after end of the cavity as follows.

3. Kinematic condition on the cavity surface:

$$\frac{DF}{Dt}=0, \text{ on the cavity surface } S_C \tag{6}$$

where $F(x,y)$ is a function expressing the cavity surface.

4. Dynamic condition on the cavity surface:

$$p=p_v, \text{ on the cavity surface } S_C \tag{7}$$

where p_v is the pressure inside the cavity.

5. Cavity closure condition:

$$t^c(x)=0, \text{ at the after end of the cavity.} \tag{8}$$

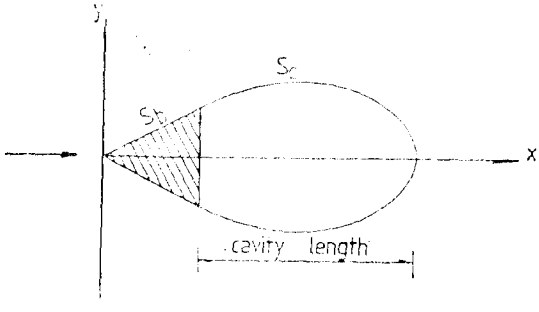

Fig. 1 Sketch of the strut and cavity boundary surface

In the case of super-cavity, a detachment condition of some form is required at the trailing edge of the strut to set the cavity shape and the circulation, Γ, around the strut in place of the Kutta condition.

6. Detachment condition at the trailing edge of the strut:

$$\lim_{A\to T,E} \hat{t}_A\cdot\nabla\Phi=\lim_{B\to T,E} \hat{t}_B\cdot\nabla\Phi \tag{9}$$

where $\hat{t}_A$ and $\hat{t}_B$ are tangential unit vectors at the strut and cavity surfaces across the trailing edge of the strut, respectively. More discussions on this are given in section 4 (see Fig. 2)

It is shown in Breslin et al.[2] that the flow tangency condition (5) may be replaced by the condition that the flow interior to the body doesn't exist, i.e., the inner velocity potential is zero

$$\Phi^-(x)=0, \text{ inside the boundary } S_{B\cup C} \tag{10}$$

where the negative sign denotes that the velocity potential is to be calculated on the interior to the strut and the cavity boundary.

Using the Bernoulli equation, we get a relation between the surface pressure, p, the tangential velocity, $\underline{V}_t$, the cavitation number, σ_v, and the pressure coefficient, C_p, as follows:

$$C_p=\frac{p-p_\infty}{\frac{1}{2}\rho U_\infty^2}=1-\left(\frac{|\underline{V}_t|}{|\underline{U}_\infty|}\right)^2,$$

on foil/cavity surface (11)

$$\sigma_v\equiv\frac{p_\infty-p_v}{\frac{1}{2}\rho U_\infty^2}=-C_{p_v}=\left(\frac{|\underline{V}_t|}{|\underline{U}_\infty|}\right)^2-1,$$

on the cavity surface (12)

where p_∞ is the ambient pressure.

According to (11) and (12), the dynamic condition on the cavity surface (7) can be replaced by the kinematic condition that $|\underline{V}_t|$ is constant, i.e.,

$$|\underline{V}_t|=\text{const.} \tag{13}$$

In this study, we are interested in the tangential velocity from which we can derive distributions of pressure.

If the pressure on the free stremline is equal to the ambient pressure, it is clear that the length of the cavity is finite, i.e., the cavity length depends on the cavitation number, σ_v. The cavity length should, therefore, be obtained through an iterative process as a part of solution to the boundary value problem. With the method of singularity distribution in mind, we have to assume a cavity length which is not known a priori. The pressure along the cavity surface and hence the cavitation number are computed using this assumed cavity length. The computed cavitation number, $\sigma_{v,\text{comp}}$, will then be compared with the prescribed cavitation number, σ_v.

Thereby we get the corresponding tangential velocity, $\underline{V}_t$, the cavitation number, σ, the lift coefficient, C_L, the cavity volume, the cavity shape and the drag coefficient, C_D.

3. Method of Distribution of Singularity

Let's consider the piecewise constant distribution of the sources and normal dipoles on the strut and cavity surface for analyzing the boundary value

problem described so far.

Velocity potentials induced by distributed sources and normal dipoles are

$$\phi_s \equiv \int \frac{q(s)}{2\pi} \log r ds, \tag{14}$$

$$\phi_d \equiv \int \frac{\mu(s)}{2\pi} \frac{\partial}{\partial n_\xi} \log r ds, \tag{15}$$

where $r=\underset{\sim}{x}-\underset{\sim}{\xi}$, $r=|\underset{\sim}{r}|$ and, $q(\xi)$, $\mu(\xi)$ are strengths of distributed sources and normal dipoles, respectively, and $\underset{\sim}{x}$, $\underset{\sim}{\xi}$ denote position vectors of field points and singular points, respectively, and log throughout this paper denotes natural logarithm.

Due to the characteristics of singularities, governing equation (3) and quidscence condition (4) are sutomatically satisfied. We may express the internal flow by means of the distribution of sources on the cavity surface and normal dipoles on both the strut and the cavity surfaces as follows:

$$\Phi_x^- = \underset{\sim}{U} \cdot \underset{\sim}{x} + \int_{S_C} \frac{q}{2\pi} \log r ds + \int_{S_B \cup S_C} \frac{\mu}{2\pi} \frac{\partial}{\partial n} \log r dt, \tag{16}$$

where S_B and S_C denote the body surface and the cavity surface, respectively.

Since the left hand side of (16) is known, (16) becomes an integral equation for unknown source and normal dipole distributions.

Equation (13), derived from the dynamic boundary condition on the cavity surface (7), implies that the velocity potential on the cavity surface has a linearity, so that we can set

$$\Phi^+ = \Phi^+_{ste} + |\underset{\sim}{U}_t| \int_0^s ds, \tag{17}$$

where Φ^+_{ste} denotes the velocity potential at the trailing edge of the strut.

Equation (17) relates the tangential velocity on the cavity surfade to the velocity potential, which is valuable and compact in its form.

The source strength representing the thickness of the cavity can be written as the product of the oncomming velocity and the first derivative of cavity thickness as in the case of thin wing theory,

$$q = v = |\underset{\sim}{U}_\infty| \frac{dt^c}{ds}, \tag{18}$$

where v is the y-component of the induced tangential velocity on the cavity surface.

Integrating the above equation, we get an expression for the cavity thickness and then an altenative form of the cavity closure condition (8),

$$t^c(l) = \int_0^s \frac{q}{|\underset{\sim}{U}_\infty|} ds = 0. \tag{19}$$

4. Detachment Condition at the Trailing Edge of the Strut

In 1911, Brillouin[3] suggested following physical conditions to determine the free streamline in the case of inviscid approximation.

1. The free streamlines are simple curves which do not intersect the body or each other.

2. The minimum pressure in the steady cavity flows is obtained only on the free streamline.

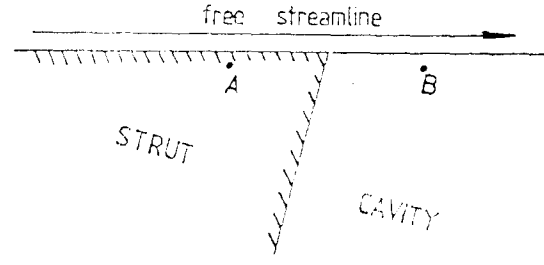

Fig. 2 Local trailing edge flow for supercavitating strut.

According to the maximum and minimum principle, if the velocity posential Φ is continuous in a closed bounded region and is analytic and not constant in the interior of the concerned domain, the modulus of the function has a minimum or maximum value on the boundary of that region.

On the other hand, the second condition tells us that the free streamline is concave to the flow. It then follows that, in the limiting case of $\sigma \to 0$, the cavity becomes infinitely long and the free streamline can be shown to tend asymptotically to a parabola near the point of infinity.

However, following Wu[14], the first order inviscid approximation for the curvature of the free streamline, κ_c, and the body boundary, κ_b, can be expressed as follows:

$$\kappa_c=-\frac{1+t^2}{2t}\left\{\frac{a_1}{b_1}-\frac{2it}{1-t^2}+\frac{2a_2}{b_1}+O(|t+1|^{\mu})\right\}$$
(as $t\to1$ along $|t|=1$) (20)

$$\kappa_b=e^{-T}\left\{\frac{2a_2}{b_1}-\frac{1+t^2}{2t}+O(|t+1|)^{\mu})\right\}$$
(as $t\to1$ along real t) (21)

where t is a complex number and a, b are complex constants. The interval, $0<t<1$, represents the body and $t>1$ is the cavity on the real axis.

Hence the curvature of the free streamline, κ_c, is infinite at $t=1$ if $a_1\neq0$ and finite if $a_1=0$. In the latter case, since the two curvatures are equal,

$$\kappa_c=\kappa_b=-\frac{2a_2}{b_1} \tag{22}$$

The above result states that the curvature of a free streamline at the starting point of cavity is either infinite or equal to the slope of the body. But the cavity shape of the former is concave to the flow or has to have a stagnation point at the starting point of the cavity, whereas that of the latter is convex and has no stagnation point on the boundary except at the after end of the cavity. Thus, according to the second condition of Brillouin, the slope of the streamline at the starting point of the cavity is equal to that of the body.

In this study, for the numerical analysis of the cavity, we represent the detachment condition at the trailing edge of the strut as an alternative form of (9). As shown in (18), there exists a linear relation between the slope of the cavity and the source strength.

Since the slope of the cavity at the starting point of the cavity can be determined from the body slope, the source strength at that point is obtained from (18) as follows:

$$q_1=U_\infty\frac{\partial}{\partial x}f(x,y), \tag{23}$$

where q_1 is the source strength at the starting point of the cavity and $f(x,y)$ denotes the function expressing the body surface.

5. Review of Classical Models for the Cavity After End

A closed body with constant pressure—and hence constant velocity—around its surface can't exist in exact potential flow but exists in a form of elliptical body within the linear theory. Thus, it is necessary to impose a termination condition at the after end of the cavity for the purpose of terminating the cavity.

The shape of the after end of the cavity has a negligible small effect on the lift, however, it plays a major role on the drag which is due to the existence of the cavity.

Some of the most important and commonly used models forming the finite cavity length, as shown in Fig. 3, are discussed below. We note that, in the potential flow approximation, the flow energy can't be removed to simulate the dissipation without simultaneous removal of the momentum or mass. For this reason, any termination condition or devices can't provide a good description of the far region from the body at all whereas they will have validity near the body.

1. Reentrant Jet Model

This model is suggested by Kreise[8], Efros[5] and Gilbarg et al.[6] independently. According to this model, there exists a sink of infinite strength behind the body so that the bounding free streamlines reverse their direction at the after end of the cavity to form a jet. The jet is assumed not to be in contact with the body by the sink.

In reality, the flow like the reentrant jet can be observed near the after end of the cavity. Due to

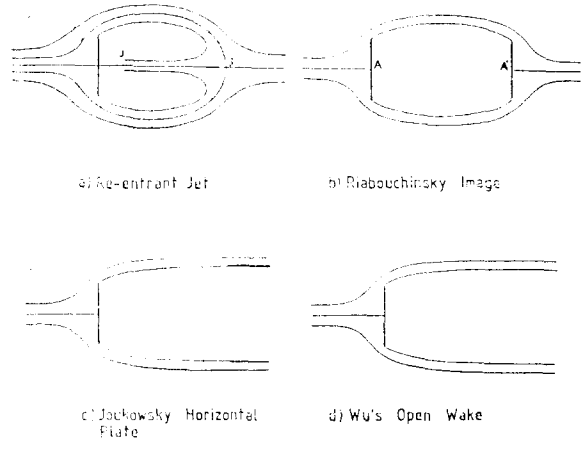

Fig. 3 Cavity termination models.

this resemblance, although being crude, this model is favored in many theoretical studies.

2. Riabouchinsky Image Model

In the Riabouchinsky image model, an image of the body is introduced at a finite distance from the body downstream to make the cavity close. The image is placed nomal to the upstream.

The total force acting on the pair of bodies is zero by the d'Alembert paradox, since the flow outside the body and the cavity is irrotational. However, the force acting on the real body alone is not zero.

This model has a merit of easiness in implementation compared to the reentrant jet model, especially in numerical analysis.

3. Wu's Open Wake Model

Wu's open wake model is a modification of Joukowsky's horizontal plate termination model. Joukowsky's horizontal plate model introduces introduces two fixed flat plates parallel to the on-coming velocity at the lower and upper points where the cavity has a maximum thickness to make the pressure gradually increase, finally reaching the ambient pressure.

As to the wake, the flow past the viscous wake region consists of two parts, which is classified by the flow pattern. In the near wake region which starts from the separation point and ends at an undetermined point, the free streamline bounding the wake and ambient flow is assumed as a streamline along which the pressure has a coustant value. But, in the far wake region, the flow is described by the potential flow so that the pressnre continuously increases up to the value of upstream and hence the far wake region is represented as a half body.

Wu[14] extended this model to the cavity problem noticing the fact that there are sometimes bubble cavities and the wake boundary line is a free streamline as observed in the case of cavity flow. The wake boundary line with bubble cavities can be assumed as a cavity boundary under the corresponding pressure coefficient. But, the distinct difference between the wake flow and cavity flow is the densities inside thd cavity and wake.

6. Linear Termination Model of the Cavity

The final target of our study is to predict hydrodynamic characteristics of marine propellers with super-cavity and partial cavity. The termination models quoted in the previous section have some merits in the two dimensional problem. However, in the case of unsteady and three dimensional hydorfoils or marine propellers, it is difficult, in the practical sense, to apply various kinds of termination models.

Moreover, in the reentrant jet model and Riabouchinsky image model, the drag is proportional to the gab of the jet and the width of the wall in each model. For this reason, the cavity may be said to be closed to the first-order.

As to Wu's open wake termination model, the wake displacement thickness generally decreases continuously from the region right behind the body up to the far downstream asymptotically. Experiments indicate that the effective thickness of the wake occupied by the bubbles is the same order as the gab of the the theoretical reentrant jet model or width of the wall in the Riabouchinsky image model. These phenomena cannot be described properly by the potential flow.

For the above reasons, we assume that the shape of the after end of the cavity terminates linearly.

The linear termination model by Lee[10] states that the cavity shape is dependent only on the source strength and the sum of strengths of sources must be zero to form a closed body.

To apply Lee's linear termination model, it is necessary to preset the stagnation point at the after end of the cavity as in the case of real flow around a thick round trailing edge. This is a dominant factor in asymmetric flow problem. In symmetric flow, the stagnation point may be coincident with the after end point of the cavity.

By observing the fact that the velocity on the cavity surface is constant, except at the after end of the cavity, we may expect that the final cavity shape will be elliptic, being exact to the first order. The non-linear cavity shape may therefore be found

with minimum number of iterations when the cavity geometry is initially assumed to be elliptic. The advantage of this so-called elliptic cavity shape approximation will be evaluated by the numerical experiments.

7. Discretization of Singularities and Solution Procedure

Distributing the discretized sources and normal dipoles on the surface of the strut and the cavity, we can express the total velocity potential as follows. Now, assume that strengths of source and normal dipole of a panel is constant along the panel, i.e.,

$$\mu(s)=\mu_j, \text{ on panel } j \tag{24}$$

$$q(s)=q_k, \text{ on panel } k \tag{25}$$

The total potential at the control point of the i-th panel is

$$\Phi_i^-=U_\infty\cdot\underline{x}_i+\sum_{k=1}^{N^S}\frac{q_k}{2\pi}\int_{\text{panel}_k}\log r ds + \sum_{j=1}^{N^D}\frac{\mu_j}{2\pi}\int_{\text{panel}_j}\frac{\partial}{\partial n}\log r ds, \quad i=1,2,\cdots,N^D \tag{26}$$

where N^D and N^S denote the number of dipole and source panels, respectively.

The above relation can be rewritten according to the termination model used at the after end of the cavity.

Applying the detachment condition at the trailing edge of the strut, the source strength just behind the base of the strut can be calculated from the slope of the strut at that point, and hence (26) is may be written as

$$0=\Phi_i^-=U_\infty\cdot\underline{x}_i+\frac{q_1}{2\pi}\int_{\text{panel}_1}\log r ds + \frac{q_{N^S}}{2\pi}\int_{\text{panel}_{N^S}}\log r ds + \sum_{k=2}^{N^S-1}\frac{q_k}{2\pi}\int_{\text{panel}_k}\log r ds + \sum_{j=1}^{N^D}\frac{\mu_j}{2\pi}\int_{\text{panel}_j}\frac{\partial}{\partial n}\log r ds \tag{27}$$

Due to the symmetry of the present problem, the number of singularity panels of unknown strengths will be reduced by half. The total velocity potential at the control point of the j-th source panel along the upper surface of the cavity in the streamwise direction can be expressed as follows:

$$\Phi_j^+=\Phi_{\text{ste}}^++|\underline{V}_t|\cdot\sum_{k=1}^{j}\Delta s_k, \quad j=1,2,\cdots,N^S/2. \tag{28}$$

Since $\Phi_j^+=\Phi_j^-=\mu_j=-\mu_j$, the above relation becomes

$$-\mu_{\text{ste}}+\mu_j+|\underline{V}_t|\cdot g_j=0 \tag{29}$$

where

$$g_j=\sum_{k=1}^{j}\Delta s_k, \tag{30}$$

and g_j represents the girth from the starting point of the cavity up to the j-th source panel.

Equation (29) shows that strengths of normal dipoles on the cavity surface can be expressed as a linear function of the tangential velocity $|\underline{V}_t|$, i.e., there is no additional unknown dipoles on the cavity surface.

Upon discretization, the cavity closure condition (19) will be recast as

$$\sum_{k=1}^{N^S/2}q_k\Delta s_k=0. \tag{31}$$

Equation (27), (29) and (31) will now form a system of linear simultaneous equations, which may be solved with the aid of a mathematical library function built in computer.

Once strengths of normal dipoles and sources are found, the new fuction for the modification of the cavity thickness is computed with (19) and added in normal direction to the previous cavity surface. The singularities will then be located on the newly determined strut and cavity surfaces to form a new boundary value problem. This process to find out the cavity geometry is iterated until a sufficient convergence is obtained. Computations of the pressure distribution, cavity shape and drag coefficient will then be followed.

8. Numerical Calculations and Discussions

As shown in Fig. 4, for the numerical analysis, we are to discretize the surface of the strut by half cosine spacing method along the x-axis, whereas we discretize the surface of the cavity by spacing equally along the x-axis with the x-component of the length of the strut panel adjacent to the trailing

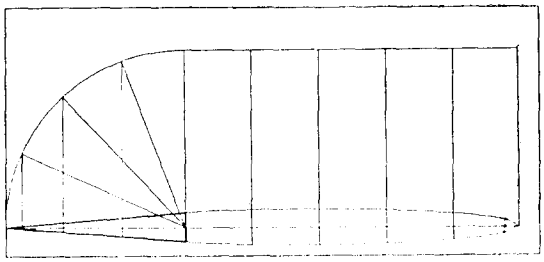

Fig. 4 Paneling of the strut and the cavity surfaces

edge.

Spacing of the cavity surface with a length leads to some deviation in drag. However, as mentioned in the previous section, we have intentions to developthis symmetric super-cavity program(SYMMCAV) up to the level of analyzing the problem of unsteady and three dimensional hydrofoil, thus, it is necessary for the purpose of saving the memory size and time to discretize the cavity and the wake by equal spacing method.

Numerical calculations have been performed for the linear termination model, Riabouchinsky's image model, and elliptical termination model with varying the cavity length from 1.8 to 4.6 times chord length and the base of the strut from 4% to 60% of the chord.

Especially, in Riabouchinsky's image model, we introduce a wall whose width is 50% of the base of the strut instead of the exact image as in the case of Uhlman[13].

In all cases, 5-iterations were carried out to ensure the convergence. The number of panels on the surface of the strut was set to 20 and the number of panels on the surface of the cavity was determined according to the cavity length. If we formulate the boundary value problem using the elliptical termination model, we could obtain fine result without resorting to any iterative process.

The SYMMCAV produces the cavitation number, σ, distributions of the pressure coefficient, C_p, the tangential velocity, V_t, and strengths of sources and normal dipoles, and the drag coefficient, C_D, for the strut.

All of the results calculated by SYMMCAV

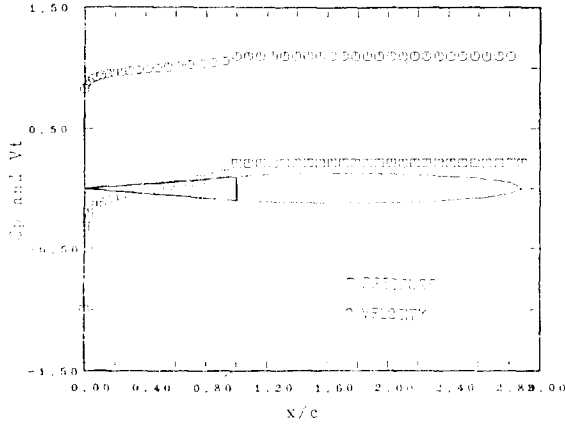

Fig. 5 Pressure and Velocity distribution, linear termination model, *Base/Chord*=0.2, Iterations=5, *Cavity-length/Chord*=1.883

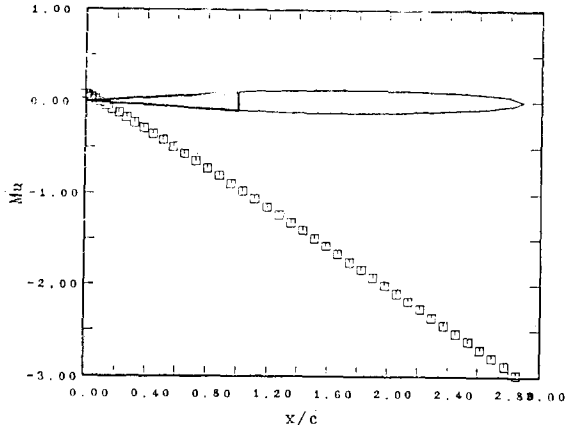

Fig. 6 Dipole Distribution, linear termination model, *Base/Chord*=0.2, Iterations=5, *Cavity-length/Chord*=1.883

were compared with the analytical solutions of Newman[12], Cox[4] et al. and Acosta[1].

Fig. 5, 7 and 9 show the cavity shape and distributions of pressure and tangential velocity in the case that the cavity length is 1.8330 times chord length and the base of the strut is 20% of the chord when using the linear termination model, Riabouchinsky's wall and elliptical termination model, respectively. In those figures, we can see that the pressure and the tangential velocity are constant along the surface of the cavity and there exists a stagnation point at the after end of the cavity which might be considered to cause reentrant jet.

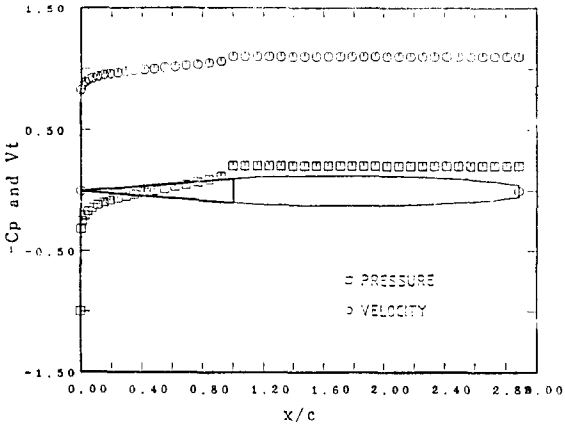

Fig. 7 Pressure and Velocity distribution, Riabouchinsky termination model, *Base/Chord*=0.2, Iterations=5, *Cavity-length/Chord*=1.883

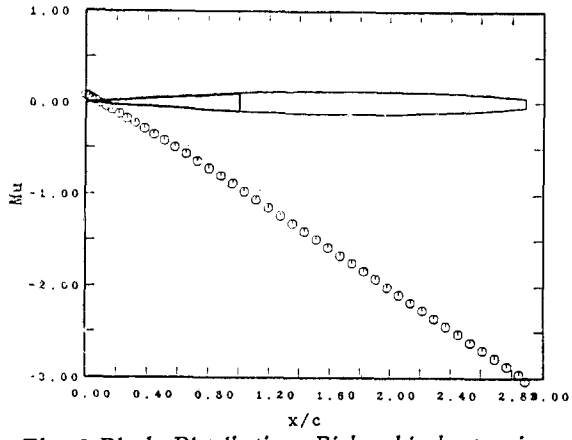

Fig. 8 Dipole Distribution, Riabouchinsky termination model, *Base/Chord*=0.2, Iterations=5, *Cavity-length/Chord*=1.883

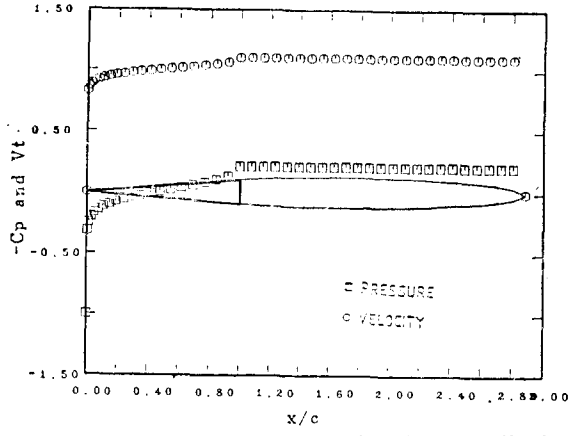

Fig. 9 Pressure and Velocity distribution, elliptic termination model, *Base/Chord*=0.2, Iterations=1, *Cavity-length/Chord*=1.883

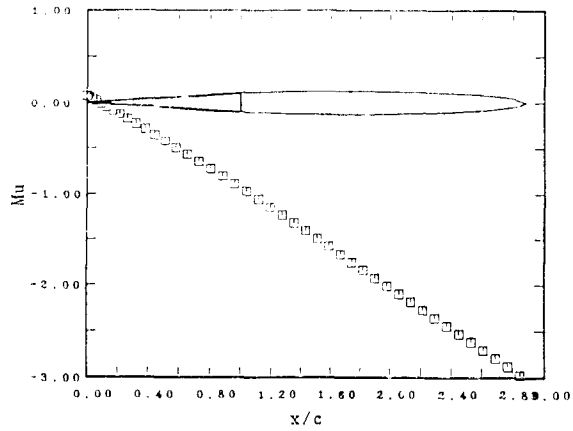

Fig. 10 Dipole Distribution, elliptic termination model, *Base/Chord*=0.2, Iterations=1, *Cavity-length/Chord*=1.883

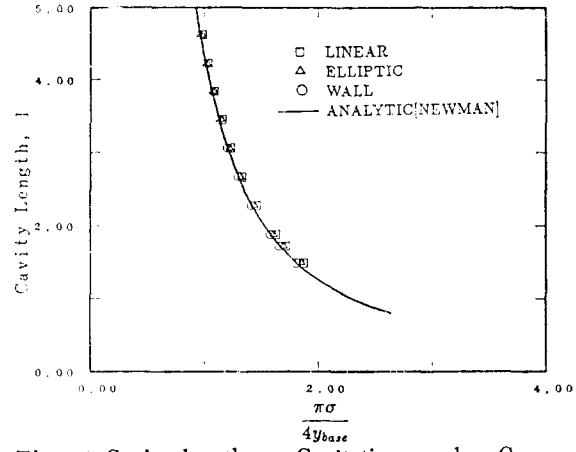

Fig. 11 Cavity length vs. Cavitation number, Comparison of cavity termination model, *Base/Chord*=0.04

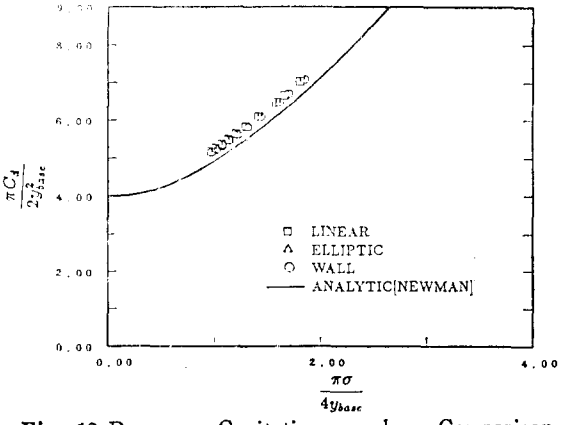

Fig. 12 Drag vs. Cavitation number, Comparison of cavity termination model, *Base/Chord*=0.04

These results are coincident with the kinematic and the dynamic boundary condition on the surface of the cavity and physical phenomena.

Fig 6, 8 and 10 show the distribution of strengths of normal dipoles under the same condition as the previous figures. Strengths of normal dipoles have a linearity along the surface of the cavity, but somewhat distorted, which is due to the difference in the girth length of the cavity panels.

In Figs. 11 and 12, we compared the cavitation number, σ, and the drag coefficient, C_D, calculated by SYMMCAV with analytical solutions (see Newman[12]) under the condition that the base width of the strut is 4% of the chord. The drag coefficient, C_D, has about 5% deviation from the analytical solution regardless of the cavity length. This deviation may be due to the fact that the girth length of the after end of the cavity.

Figs. 13 and 14 show the cavitation number, σ, and the drag coefficient, C_D, calculated by SYMMCAV compared with the analytical solutions when the base width of the strut is 20% of the chord.

In Fig. 15, the shapes of the after end of the cavity using the corresponding termination model are compared each other.

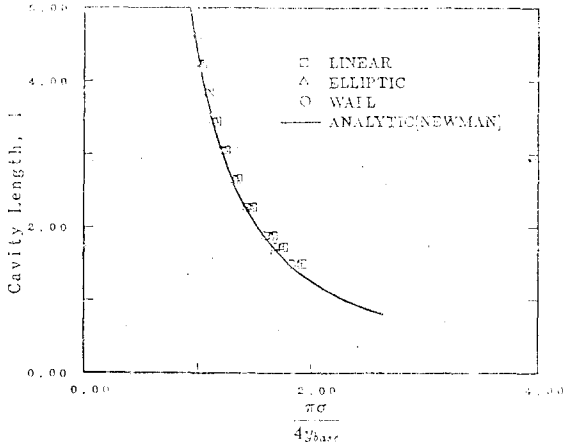

Fig. 13 Cavity length vs. Cavitation number, Comparison of cavity termination model, *Base/Chord*=0.2

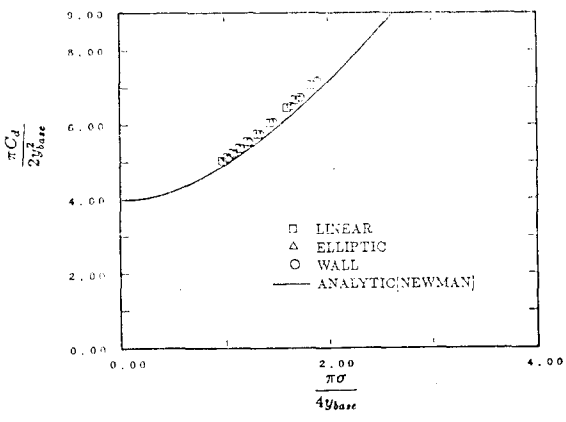

Fig. 14 Drag vs. Cavitation number, Comparison of cavity termination model *Base/Chord* =0.2

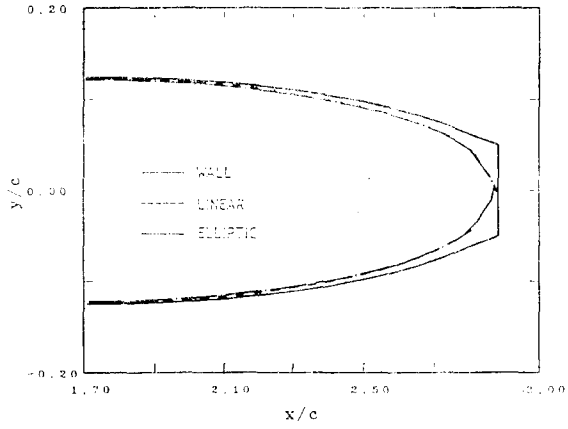

Fig. 15 Comparison of geometry of the after end of the cavity, *Base/Chord*=0.04, *Cavity-length/Chord*=1.883, *Base/Chord*=0.04

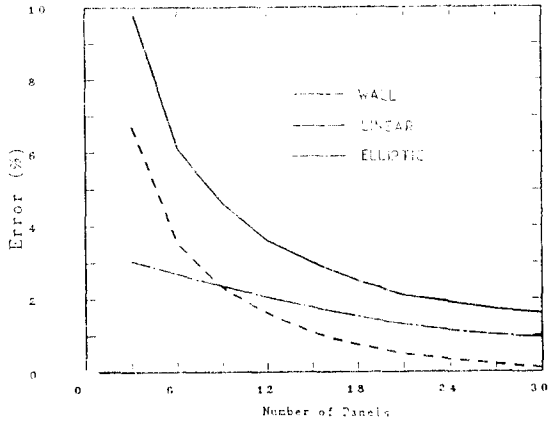

Fig. 16 Convergence Test, Comparison of cavity termination model, *Cavity-length/Chord* =3.0 *Base/Chord*=0.04

The results of convergence test under the condition that the cavity length is 1,830 times chord length and the base of the strut is 4% of the chord with varying the number of panels is presented in Fig. 16. As shown in Fig. 16, the final difference of the cavitation number calculated by SYMMCAV using 30 elements on the surface of the strut is less than 1.6% compared with the analytical solution.

9. Conclusions

1. A potential-based surface panel method is formulated for the solution of a super-cavitating flow problem about a 2-dimensional symmetric strut. The method employs the normal dipole and source distributions on the strut and the cavity surfaces.

2. The detachment condition at the interface of the strut base and trailing cavity is found important.

3. The elliptical cavity shape, which is an exact solution to the linearized cavity flow problem, provides an excellent initial approximation to the converged cavity shapes, minimizing the the necessity of time-consuming iterations.

4. Numerical computations show a good correlation with the analytical solutical solution, at least the case of linear symmetric flows.

5. Experimental data and results of non-linear theory on the super-cavity problem are rare. Comparing the present non-linear numerical results with the analytical results of linear theory shows a small discrepancy between them.

10. Acknowledgement

The authors are grateful to the valuable comments and discussions of Prof. S.J. Lee of CNU and Drs. J.T. Lee and C.G. Kang of KRISO.

Sincere thanks are extended to financial support of Hyundai Maritime Research Institute.

References

[1] Acosta, A.J., "A note on partial cavitation of flat plate hydrofoils", Calif. Inst. Technol. Hydrodyn. Lab. Rept. No. E-19.9, Pasadena, Cal., 1955.

[2] Breslin, J.P., Van Houten, R.J., Kerwin, J.E., Johnsson, C.A., "Theoretical and Experimental Propeller-Induced Hull Pressures Arising from Intermittent Blade Cavitation, Loading, and Thickness", *SNAME Trans.*, Vol. 90, 1982.

[3] Brillouin, M., "Les surfaces de glissement de Helmholtz et la resistance des fluides", Ann. Chim. Phys. 23, pp.145-230, 1911.

[4] Cox, A. and Clayden, W., "Cavitating flow about a wedge at incident", *J. Fluid Mech.* 3, pp.615-617, 1958.

[5] Efros, D., "Hydrodynamical theory of two dimensional flow with cavitation", Dokl. Akad. Nauk SSSR 51, pp.267-270, 1946.

[6] Gilbarg, D. and Rock, D., "On two theories of plane potential flows with finite cavities", Naval Ord. Lab. Memo. 8718, 1946.

[7] Hess, J.L., & Valarezo, W.O., "Calculation of Steady Flow about Propellers using a Surface Panel Method", *J. Propulsion*, Dec. 1985.

[8] Kreisel, G., "Cavitation with finite cavitation number", Admiralty Res. Lab. Rept. No. R1/H/26, 1946.

[9] Lee, C.S., "Prediction of Steady and Unsteady Performance of Marine Propellers with or without Cavitation by Numerical Lifting Surface Theory", Ph.D. Thesis, Department of Ocean Engineering, M.I.T., Cambridge, Mass., 1979.

[10] Lee, C.S., "A Potential-based Panel Method for the Analysis of a 2-dimensional Cavitating Hydrofoil", College of Engineering, C.N.U., Daejeon, Korea, 1989.

[11] Lee, J.T., "A Potential-based Panel Method for the Analysis of Marine Propellers in Steady flow", Ph.D. Thesis, Department of Ocean Engineering, M.I.T., Cambridge, Mass., 1987.

[12] Newman, J.N., "Marine Hydrodynamics", The MIT Press, Cambridge, Mass., 1977.

[13] Uhlman, J.S., "The Surface Singularity or Boundary Intergral Method Applied to Super-cavitating Hydrofoils", *J. of Ship Research*,

Vol. 33, No. 1, March 1989, pp. 16-20.

[14] Wu, T.Y., "Cavity and Wake Flows", Annual Review of Fluid Mechanics, Vol. 4, pp. 243-284, 1972.

[15] Yang, C.I. & Jesup, S.D., "Benchmark Analysis of a Series ofsPropellers with a Panel Method", *SNAME Popeller '88 Symp.*, Virginia Beach, VA, 1988, pp. 17/1-10.